Emergence of a Novel Pseudogap Metallic State in a Disordered 2D Mott Insulator

Elias Lahoud,[1] O. Nganba Meetei,[2] K. B. Chaska,[1] A. Kanigel,[1] and Nandini Trivedi[2]
[1]*Physics Department, Technion-Israel Institute of Technology, Haifa 32000, Israel*
[2]*Department of Physics, The Ohio State University, Columbus, Ohio 43210, USA*
(Received 18 April 2013; revised manuscript received 5 August 2013; published 21 May 2014)

We explore the nature of the phases and an unexpected disorder-driven Mott insulator to metal transition in a single crystal of the layered dichalcogenide 1T-TaS_2 that is disordered without changing the carrier concentration by Cu intercalation. Angle resolved photoemission spectroscopy measurements reveal that increasing disorder introduces delocalized states within the Mott gap that lead to a finite conductivity, challenging conventional wisdom. Our results not only provide the first experimental realization of a disorder-induced metallic state but in addition also reveal that the metal is a non-Fermi liquid with a pseudogap with a suppressed density of states that persists at finite temperatures. Detailed theoretical analysis of the two-dimensional disordered Hubbard model shows that the novel metal is generated by the interplay of strong interaction and disorder.

DOI: 10.1103/PhysRevLett.112.206402 PACS numbers: 71.30.+h, 61.43.Bn, 79.60.Ht

The interplay of disorder and strong correlations and the resulting quantum phase transitions are long-standing problems and continue to be major areas of research in condensed matter physics today [1–9]. Mott insulators at commensurate filling emphasize the role played by repulsive interactions in localizing electrons. These insulators have a gap to charge excitations and are often associated with magnetic order and low lying spin excitations [10–12]. On the other hand, Anderson insulators describe noninteracting electrons in a random potential, which show a mobility gap but have gapless single particle excitations and no magnetic properties [13,14]. The overarching question we ask in this Letter is the effect of disorder on the charge and spin excitations of a Mott insulator as illustrated in Fig. 1. A major challenge is to find strongly correlated quantum materials where disorder can be introduced in a controlled manner without changing the carrier concentration. The layered dichalcogenide 1T-TaS_2 with Cu intercalation is an excellent candidate for exploring precisely this interplay between strong correlations and disorder.

The transition-metal dichalcogenide 1T-TaS_2 is a quasi-2D system with a very rich phase diagram. Upon decreasing the temperature it undergoes several charge density wave (CDW) phase transitions [15]. It even becomes superconducting when subjected to external pressure or chemical doping [16,17].

In this joint experiment and theory collaboration, we focus on the commensurate CDW (CCDW) phase below $T = 180$ K, shown to be a Mott insulator, and explore the effect of disorder without doping introduced by intercalating Cu. Using detailed angle resolved photoemission spectroscopy (ARPES) data along with transport measurements we show that a novel disorder induced metal is realized. It has surprising non-Fermi liquid behavior characterized by a temperature dependent pseudogap in the spectral function as shown in Fig. 3. Our theoretical analysis of the disordered Hubbard model reveals the origin of the extended states in the Mott gap and the pseudogap in the spectral function as summarized in Fig. 4.

The pseudogap, a state showing suppression in the density of states, has emerged as a new state of matter in very different systems though suggesting very different origins. By now it has been shown to arise due to pairing correlations persisting in the normal state [18–20], due to competing spin and charge orders [21], as well as due to a disorder-generated hard gap and pseudogap in superconducting thin films [22–26]. Our discovery here is

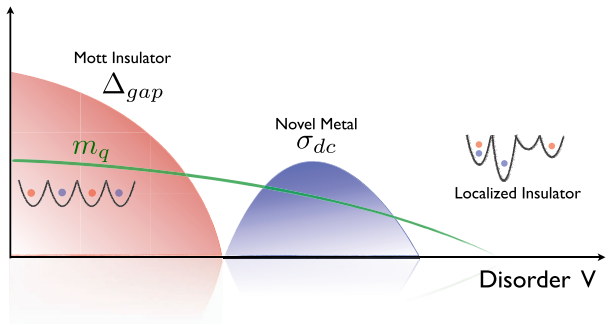

FIG. 1 (color online). Schematic figure showing the effect of disordering a Mott insulator (without adding carriers). As the disorder strength V is increased relative to the bandwidth, the charge gap Δ_{gap} in the Mott insulator vanishes at the quantum phase transition to a metal. The novel metal has a finite dc conductivity σ_{dc} and other unusual spectral properties elucidated by angle resolved photoemission spectroscopy experiments reported here. At higher disorder we expect a second quantum phase transition from the metal to a gapless localized insulator. If the Mott insulator has magnetic order m_q, it need not be tied to the metal insulator transitions.

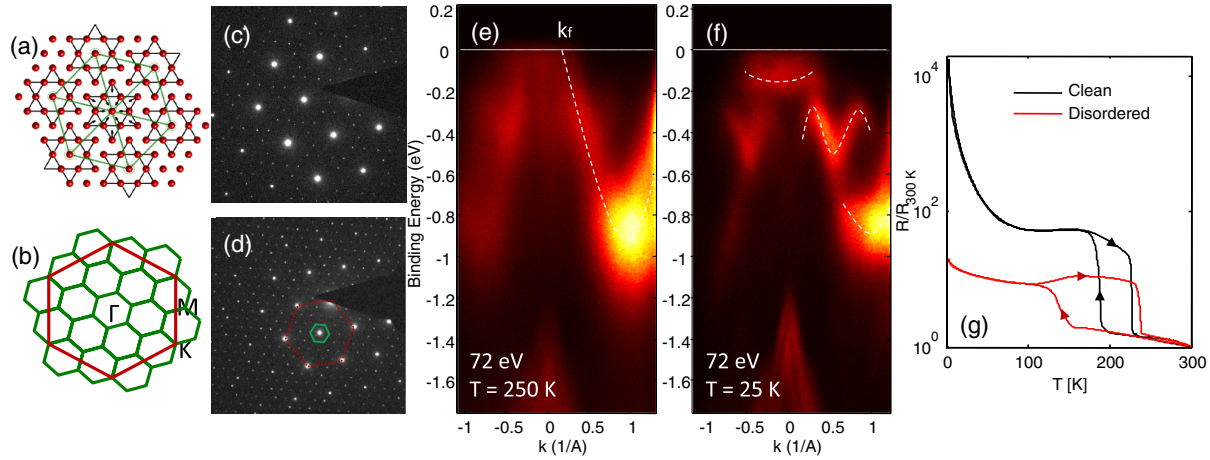

FIG. 2 (color online). Mott phase in 1T-TaS_2: (a) visualization of the CCDW phase and star-of-David clusters on a triangular lattice. (b) The 2D Brillouin zone of the original triangular Ta sheet (red), and the CCDW phase reconstructed reciprocal unit cells (green). (c), (d) TEM diffraction images from a disordered sample in the nearly commensurate CDW phase ($T = 223$ K) and the commensurate CDW phase ($T = 123$ K), respectively. (e),(f) ARPES data from a disordered sample showing the band dispersion along the Γ-M direction above and below the CCDW phase transition at 180 K, respectively. The dashed lines are guides to the eye showing the band dispersion. (g) In-plane resistance as a function of temperature for a clean and a disordered sample upon cooling from 300 K down to 2 K and heating back to 300 K. 1T-TaS_2 is quasi-2D with large resistance anisotropy ($\rho_c/\rho_a \approx 500$) [27,28]. For a discussion of the unusual temperature dependence of the resistivity, see the Supplemental Material [29].

significant because it points to yet another factor, Coulomb correlations and Mott physics, driving the dominant mechanism for a pseudogapped metallic state in Cu-intercalated 1T-TaS_2.

1T-TaS_2 *(single band Mott insulator).*—We start by establishing that 1T-TaS_2 is a single orbital Mott insulator. Despite the seemingly complicated electronic properties, 1T-TaS_2 has a simple crystal structure composed of weakly coupled layers, each layer containing a single sheet of tantalum atoms, sandwiched in between two sheets of sulfur atoms. The Ta atoms within each layer form a 2D hexagonal lattice. The basic CDW instability is formed within the tantalum layers by the arrangement of 13 Ta atoms into a "star-of-David" shaped cluster [Fig. 2(a)]. As temperature is lowered, the size of the CDW domains becomes larger until all the domains interlock into a single coherent CDW modulation extending throughout the layer in the CCDW phase below $T_{\mathrm{CCDW}} = 180$ K. The new star-of-David unit cells form a hexagonal lattice and the corresponding reduced Brillouin zone is depicted by the small green hexagon in Fig. 2(b).

The transition into the CCDW phase is accompanied by a metal-insulator transition into a Mott phase [15,30], clearly seen from resistivity measurements shown in Fig. 2(g). In agreement with previous works [31], the structural CCDW formation also leads to an electronic reconstruction as seen from the ARPES spectra. Before reconstruction a parabolic band [dashed line in Fig. 2(e)] with a bandwidth ≈1 eV, originates from the Ta 5d orbital [32], and disperses upwards from M towards the Γ point, crossing the Fermi energy at 25% of the Γ-M distance. After CCDW reconstruction, the upper most subband, lying closest to the Fermi energy, is well separated in energy from the rest with a bandwidth of about $W \approx 45$ meV. The Coulomb on-site energy U is evaluated to be on the order of 0.1 eV [16]. Thus the low energy physics of 1T-TaS_2 is captured by a 2D single-band Hubbard model on a triangular lattice [30] with the value of $U/W \approx 2.2$ well over the critical value for the Mott transition ($U_C/W \approx 1.3$) [33].

Cu intercalation.—The presence of intercalated Cu can locally deform the crystal and the long-range strain fields [34] can lead to modifications of the electronic structure of the CCDW phase. We have modeled the effects of randomly distributed Cu on the CCDW phase by a disordered Hubbard model. The CCDW phase remains robust against this disorder (see the Supplemental Material [29]) as seen from (a) the TEM images showing similar diffraction patterns in the clean and disordered systems, (b) the large hysteresis in the temperature-dependent resistivity with a sharp transition, and (c) the formation of subbands due to Fermi surface reconstruction that persists upon intercalation.

Spectral properties of a disordered Mott insulator.—ARPES data on disordered 1T-TaS_2 [see Figs. 3(a)–3(b)] shows a significant increase of spectral weight in the [−0.1 eV, 0 eV] energy range at the Γ point. The energy distribution curves (EDCs) in Fig. 3(c) show the transfer of spectral weight towards lower binding energy in the disordered sample, with a line shape that is slightly skewed towards $E = 0$. The symmetrized EDC [Fig. 3(d)] confirms the presence of a "soft" gap, where the spectral weight at zero energy is about 20% of the intensity at the peak and the broad peaks are shifted inwards, leaving a smaller Mott gap. The filling up of the Mott gap is accompanied by an

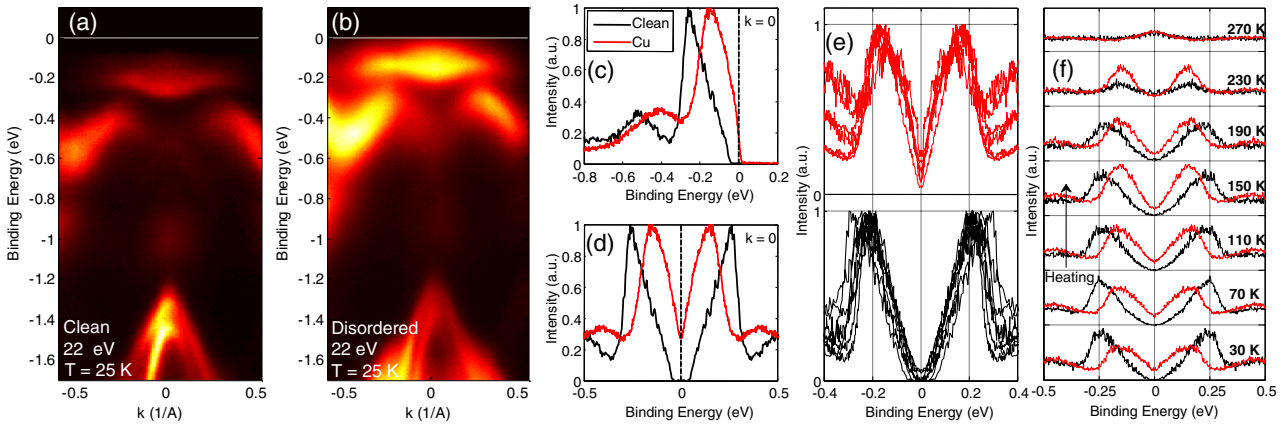

FIG. 3 (color online). ARPES spectra of a disordered Mott insulator 1T-TaS_2: spectra taken with 22 eV photons along the Γ-K direction at $T = 25\ \mathrm{K} < T_{\mathrm{CCDW}}$. Panel (a) for a clean system reveals a Mott gap as indicated by the lack of intensity within about 80 meV of the Fermi energy. Panel (b) for a disordered sample shows the presence of significant spectral weight close to the Fermi energy, inside the energy gap. In panels (c)–(f), the scans in black are for a clean system while those in red are for a Cu intercalated disordered system. (c) Comparison of the EDC at the Γ point taken from the scans in (a) and (b). The peak in the disordered 1T-TaS_2 is broadened and shifted towards lower binding energy and there is substantial intensity at zero energy. (d) The same EDCs shown in (c) after symmetrization clearly reveal the closing of the gap in the disordered sample, and the formation of a pseudogap with about 20% of the peak intensity. (e) Reproducibility of the results: EDCs from 13 different samples (seven clean and six disordered) taken in different ARPES systems with different photon energies and polarizations; all reveal the same qualitative behavior. (f) Evolution of the pseudogap at the Γ point as a function of increasing temperature. While at low temperatures the spectral weight at zero energy is much larger in the disordered samples, above the CCDW transition temperature the difference in the spectral functions of the clean and disordered samples disappears.

insulator to metal transition indicated by the drop in resistivity by several orders of magnitude [Fig. 2(g)]. The emergent metallic phase exhibits novel non-Fermi liquid characteristics like a distinct pseudogap around $\omega = 0$ and an unusual low temperature resistivity that increases slightly with decreasing temperature (discussed in more detail later). The results are highly reproducible as seen in Fig. 3(e).

The pseudogap at low temperatures is found to persist up to higher temperatures. The temperature dependence of the symmetrized EDC at Γ is shown in Fig. 3(f) for a clean and disordered sample. The difference in line shape and in the shape of the gap is most prominent at low temperatures, and the EDCs become increasingly similar as temperature is raised.

The are several points about the data that are significant. (1) Unlike in semiconductors with rigid bands, we find no evidence of disorder generating a significant amount of localized impurity states in the correlated Mott insulator. Such impurity states, if present, would have shown up above T_{CCDW} as additional spectral weight near the chemical potential in the disordered sample compared to the clean case (see the Supplemental Material [29]), which is however not observed. (2) It is also clear that phase separation and domains of the CCDW separated by metallic regions cannot explain the spectrum in the pseudogapped metal. The spectrum due to phase separation would be a weighted average of that from a Mott insulator and a normal metal, and as a result the Hubbard bands for the disordered system would remain fixed at the location of the clean system. This is inconsistent with our observations that the Hubbard bands in the disordered samples move to lower energies [Fig. 3(d)].

Disordered Hubbard model.—To gain better insight into our experimental results, we investigate the effect of disorder on a Mott insulator using a half-filled single band Hubbard model on a triangular lattice. It describes the CCDW phase of 1T-TaS_2.

$$H = -t\sum_{\langle ij\rangle,\sigma}(c^{\dagger}_{i\sigma}c_{j\sigma} + \mathrm{H.c.}) - t'\sum_{\langle\langle ij\rangle\rangle}(c^{\dagger}_{i\sigma}c_{j\sigma} + \mathrm{H.c.}) + \sum_{i,\sigma}(\epsilon_i - \mu)c^{\dagger}_{i\sigma}c_{i\sigma} + U\sum_i n_{i\uparrow}n_{i\downarrow}. \quad (1)$$

Here t is the nearest-neighbor hopping between unit cells, t' the next nearest hopping, and U is the on-site interaction strength. $c^{\dagger}_{i\sigma}(c_{i\sigma})$ creates (annihilates) an electron of spin σ at site i, and $n_{i\sigma} = c^{\dagger}_{i\sigma}c_{i\sigma}$ is the number operator for spin σ at site i. The on-site disorder potential ϵ_i is chosen from a flat distribution in the range $[-V/2, V/2]$, and captures the effect of lattice distortions due to Cu intercalation. In our analysis, we tune the chemical potential μ for each disorder realization to fix the density at half filling. We solve Eq. (1) within inhomogeneous mean-field theory. The interaction term is approximated as $n_{i\uparrow}n_{i\downarrow} \approx n_{i\uparrow}\langle n_{i\downarrow}\rangle + \langle n_{i\uparrow}\rangle n_{i\downarrow} - \langle n_{i\uparrow}\rangle\langle n_{i\downarrow}\rangle - \langle S^{+}_i\rangle S^{-}_i - \langle S^{-}_i\rangle S^{+}_i + \langle S^{+}_i\rangle\langle S^{-}_i\rangle$, where the operator $\mathbf{S} = \sum_{\sigma,\sigma'}c^{\dagger}_{\sigma}\tau_{\sigma,\sigma'}c_{\sigma'}$ and τ are the Pauli spin matrices. Due to the presence of disorder, the density

and spin fields are site dependent and the $3N$ parameters $(\{\langle n_{i\sigma}\rangle, \langle S_i^+\rangle = \langle S_i^-\rangle^*\}, i = 1, \ldots, N$ and $\sigma = \uparrow$ or $\downarrow)$, where N is the total number of sites, are obtained by a self-consistent solution of the coupled inhomogeneous Hartree-Fock equations.

At half filling in the clean limit with $t' = 0$, mean field solutions gives an insulator for $U > U_c \simeq 5.27t$ [35] along with magnetic ordering of the spins on the triangular lattice in a commensurate 120° pattern. For the rest of the calculation, we choose $U = 6t$ in order to remain in the insulating phase. Inclusion of $t' = 0.3t$ does not affect the magnetic ground state, but is important for producing a realistic band structure for comparison with experiments. We also find that small changes in filling ($\delta n < 2\%$) do not change the mean-field solution.

EDC of spectral function.—For a given disorder realization, we numerically diagonalize the mean-field Hamiltonian exactly to obtain the single particle eigenstates $\{|\Psi_\alpha\rangle\}$ and eigenvalues $\{\epsilon_\alpha\}$, which are used to calculate the single particle Green's function

$$G(\mathbf{r}_1, \mathbf{r}_2, \omega) = \sum_\alpha \frac{\langle \mathbf{r}_1|\psi_\alpha\rangle\langle\psi_\alpha|\mathbf{r}_2\rangle}{\omega + i\eta - \epsilon_\alpha}. \quad (2)$$

For a given disorder strength V, we average over several disorder realizations, and then Fourier transform to get the spectral function $A(\mathbf{k}, \omega) = -(1/\pi)\mathrm{Im}G(\mathbf{k}, \omega)$.

While previous studies have found a suppression in the total density of states around zero energy [36–38] as also shown in Fig. 4(a), here our focus is on the disorder dependence of the spectral function as highlighted in Fig. 4(b). The EDC at the Fermi momentum for different amounts of disorder agree qualitatively with our experimental results shown in Figs. 3(c) and 3(d) on several aspects: (1) With increasing disorder the Mott gap closes and finite spectral weight develops at $\omega = 0$ [see the inset of Fig. 4(b)]. (2) The shape of the gap changes from a hard U shaped gap in the clean limit to a V shaped soft gap in the disordered case. (3) The positions of the broad peaks corresponding to the upper and lower Hubbard bands move closer to the chemical potential with increasing disorder in agreement with experimental data. In general, the spectral function is asymmetric around $\omega = 0$ [39]. Since ARPES is only able to access the filled states, the experimental data have been symmetrized around $\omega = 0$.

Transport properties in the pseudogapped metallic phase.—Within the relaxation time approximation, the conductivity is given by (see the Supplemental Material [29])

$$\sigma_{xx} = 2e^2 v_F^2 \tau_F \int d\epsilon g(\epsilon)\left(-\frac{\partial f_\epsilon}{\partial \epsilon}\right), \quad (3)$$

where $g(\epsilon)$ is the density of states. A direct consequence of the strong energy-dependent $g(\epsilon)$ in the disordered

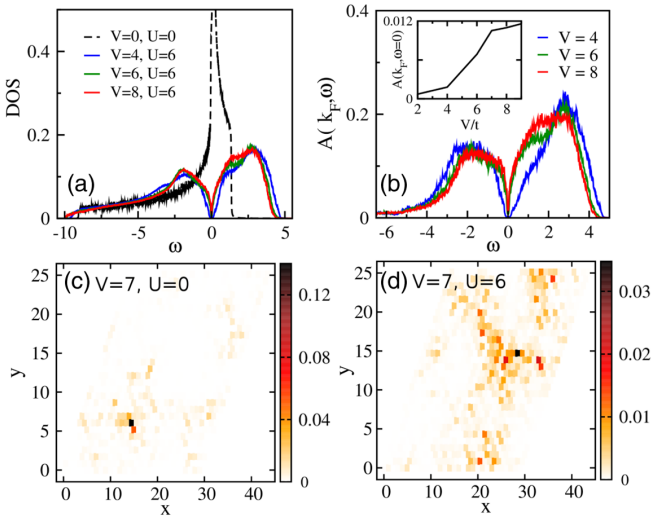

FIG. 4 (color online). (a) Theoretical density of states as a function of disorder V (in units of hopping t) for interaction $U = 6t$. (b) EDC at $k = k_F$ for $U = 6t$ showing a well formed gap for weak disorder ($V < U$), which closes for $V \geq U$ with a pseudogap persisting. Inset shows the monotonic increase of spectral weight at $\omega = 0$ with disorder. Panels (c) and (d) show the spatial map of the probability density $|\Psi(i)|^2$ of the eigenstate at $\omega = 0$ for $V = 7t$ and $U = 0$ (c) and $U = 6t$ (d). Remarkably repulsive interactions compete against disorder and delocalize the wave function over the entire lattice. The results in panels (a) and (b) are on 18×18 lattices averaged over 100 disorder realizations, and in (c) and (d) on a 32×32 lattice for a single realization.

Hubbard model is that the low temperature behavior of the resistivity $\rho(T)$ increases with decreasing temperature and eventually saturates as $T \to 0$. This then defines the characteristic transport signature in the pseudogapped metallic phase (see Fig. 3 in the Supplemental Material [29]), distinct from a Fermi liquid that has a positive temperature coefficient of resistivity and from an insulator that shows no saturation at low temperatures. Such unusual low temperature behavior has also been reported in the context of high mobility suspended graphene samples with the chemical potential tuned close to the Dirac point [40].

In conclusion, we have shown that while for noninteracting electrons disorder always localizes the wave functions, in strongly interacting systems, under certain conditions, disorder can delocalize them, quite unlike midgap states in a conventional semiconductor.

This remarkable phenomena has been demonstrated here through ARPES measurements on Cu intercalated 1T-TaS_2. We have established the first example of a non-Fermi liquid metal with a pseudogap generated upon disordering a 2D Mott insulator. In our calculation, the additional low frequency weight upon disordering the system arises primarily from k states close to the underlying Fermi surface of the tight-binding model. In the experimental data in Fig. 3(b), on the other hand, the additional weight appears from states close to the Γ point. The discrepancy could be due to

experimental resolution or possibly due to magnetic ordering and the resultant zone folding that can also push the weight close to the Γ point. While many exotic phases have been found upon doping in proximity to Mott insulators and spin liquids such as the *d*-wave superconductivity in the cuprates and organics, in all these systems doping simultaneously introduces both carriers and disorder. We have explored a regime where disorder is separately tuned without changing the carrier concentration. Our investigations open up the possibility of several future explorations of the nature of magnetism, its evolution with disorder, and its relation to the metal-insulator transitions.

O. N. M. and N. T. acknowledge support from U.S. DOE Grant No. DE-FG02-07ER46423 and the Ohio Supercomputer Center for computational resources. The Synchrotron Radiation Center is supported by NSF DMR-0084402.

[1] E. Abrahams, S. V. Kravchenko, and M. P. Sarachik, Rev. Mod. Phys. **73**, 251 (2001).
[2] S. V. Kravchenko and M. P. Sarachik, Rep. Prog. Phys. **67**, 1 (2004).
[3] S. V. Kravchenko, G. V. Kravchenko, J. E. Furneaux, V. M. Pudalov, and M. D'Iorio, Phys. Rev. B **50**, 8039 (1994).
[4] A. Punnoose and A. M. Finkel'stein, Science **310**, 289 (2005).
[5] T. Vojta, F. Epperlein, and M. Schreiber, Phys. Rev. Lett. **81**, 4212 (1998).
[6] V. Dobrosavljević, E. Abrahams, E. Miranda, and S. Chakravarty, Phys. Rev. Lett. **79**, 455 (1997).
[7] V. Dobrosavljević and G. Kotliar, Phys. Rev. Lett. **78**, 3943 (1997).
[8] D. Heidarian and N. Trivedi, Phys. Rev. Lett. **93**, 126401 (2004).
[9] V. Dobrosavljević, N. Trivedi, and J. Valles, *Conductor-Insulator Quantum Phase Transitions* (Oxford University Press, New York, 2012).
[10] P. Fazekas, *Lecture Notes on Electron Correlation and Magnetism* (World Scientific, Singapore, 1999).
[11] M. Imada, A. Fujimori, and Y. Tokura, Rev. Mod. Phys. **70**, 1039 (1998).
[12] A. Georges, G. Kotliar, W. Krauth, and M. J. Rozenberg, Rev. Mod. Phys. **68**, 13 (1996).
[13] E. Abrahams, P. W. Anderson, D. C. Licciardello, and T. V. Ramakrishnan, Phys. Rev. Lett. **42**, 673 (1979).
[14] P. A. Lee and T. V. Ramakrishnan, Rev. Mod. Phys. **57**, 287 (1985).
[15] J. Wilson, F. Di Salvo, and S. Mahajan, Adv. Phys. **24**, 117 (1975).
[16] B. Sipos, A. F. Kusmartseva, A. Akrap, H. Berger, L. Forr, and E. Tuti, Nat. Mater. **7**, 960 (2008).
[17] P. Xu, J. O. Piatek, P.-H. Lin, B. Sipos, H. Berger, L. Forró, H. M. Rønnow, and M. Grioni, Phys. Rev. B **81**, 172503 (2010).
[18] M. Randeria, N. Trivedi, A. Moreo, and R. T. Scalettar, Phys. Rev. Lett. **69**, 2001 (1992).
[19] J. C. Campuzano, M. R. Norman, and M. Randeria, in *Superconductivity*, Vol. 2 edited by K. H. Bennemann and J. B. Ketterson (Springer, New York, 2004), p. 923.
[20] J. P. Gaebler, J. T. Stewart, T. E. Drake, D. S. Jin, A. Perali, P. Pieri, and G. C. Strinati, Nat. Phys. **6**, 569 (2010).
[21] C. V. Parker, P. Aynajian, E. H. da Silva Neto, A. Pushp, S. Ono, J. Wen, Z. Xu, G. Gu, and A. Yazdani, Nature (London) **468**, 677 (2010).
[22] A. Ghosal, M. Randeria, and N. Trivedi, Phys. Rev. Lett. **81**, 3940 (1998).
[23] A. Ghosal, M. Randeria, and N. Trivedi, Phys. Rev. B **65**, 014501 (2001).
[24] K. Bouadim, Y. L. Loh, M. Randeria, and N. Trivedi, Nat. Phys. **7**, 884 (2011).
[25] B. Sacépé, C. Chapelier, T. I. Baturina, V. M. Vinokur, M. R. Baklanov, and M. Sanquer, Phys. Rev. Lett. **101**, 157006 (2008).
[26] B. Sacépé, T. Dubouchet, C. Chapelier, M. Sanquer, M. Ovadia, D. Shahar, M. Feigel'man, and L. Ioffe, Nat. Phys. **7**, 239 (2011).
[27] F. J. Di Salvo and J. E. Graebner, Solid State Commun. **23**, 825 (1977).
[28] P. D. Hambourger and F. J. Di Salvo, Physica (Amsterdam) **99B+C**, 173 (1980).
[29] See Supplemental Material at http://link.aps.org/supplemental/10.1103/PhysRevLett.112.206402 for additional information about the following: (i) Technical details about the experiment including sample preparation, ARPES measurements and discussion of experimentally observed effects of disorder. (ii) A theoretical understanding of the unusual resistivity of the pseudogapped metal.
[30] P. Fazekas and E. Tosatti, Physica (Amsterdam) **99B+C**, 183 (1980).
[31] M. H. Whangbo and E. Canadell, J. Am. Chem. Soc. **114**, 9587 (1992).
[32] K. Rossnagel and N. V. Smith, Phys. Rev. B **73**, 073106 (2006).
[33] K. Aryanpour, W. E. Pickett, and R. T. Scalettar, Phys. Rev. B **74**, 085117 (2006).
[34] A. I. Frenkel, D. M. Pease, J. I. Budnick, P. Metcalf, E. A. Stern, P. Shanthakumar, and T. Huang, Phys. Rev. Lett. **97**, 195502 (2006).
[35] H. R. Krishnamurthy, C. Jayaprakash, S. Sarker, and W. Wenzel, Phys. Rev. Lett. **64**, 950 (1990).
[36] S. Chiesa, P. B. Chakraborty, W. E. Pickett, and R. T. Scalettar, Phys. Rev. Lett. **101**, 086401 (2008).
[37] H. Shinaoka and M. Imada, Phys. Rev. Lett. **102**, 016404 (2009).
[38] R. Wortis and W. A. Atkinson, Phys. Rev. B **82**, 073107 (2010).
[39] M. Randeria, R. Sensarma, N. Trivedi, and F.-C. Zhang, Phys. Rev. Lett. **95**, 137001 (2005).
[40] K. I. Bolotin, K. J. Sikes, J. Hone, H. L. Stormer, and P. Kim, Phys. Rev. Lett. **101**, 096802 (2008).